# Finite Element Simulation of Double Diffusion in a Salt Stratified Fluid Heated from Below

**Jorge Milhazes[1] and Pedro J. Coelho[1]**

[1] IDMEC, Mechanical Engineering Department, Instituto Superior Técnico, Universidade de Lisboa, Lisbon, Portugal

**Abstract**

Transient double diffusion in a salt stratified fluid confined in a plexiglass rectangular box heated from below was experimentally investigated in a previous study aiming at a better understanding of the physics of a salinity gradient solar pond. In the present work, a finite element simulation of the transient flow dynamics is reported. The Navier-Stokes equations are solved along with the transport equations for energy and salinity. The advection terms are stabilized using a spurious oscillation at layers diminishing method and the time discretization is carried out using a second-order backward differencing scheme. The influence of lateral cooling due to heat losses to the surroundings on double diffusion is investigated. The predictions are consistent with Schlieren images and show the time evolution of the interfaces of the convective and diffusive zones. Several physical phenomena, such as the transport across a diffusive interface, the disruption of an interface and the role of lateral cooling on double diffusive convection were observed.

*Keywords: Solar ponds, Salinity gradient, Finite elements, Double diffusion*.

## 1. Introduction

Double-diffusive convection was originally described in a paper by Stommel *et al*.(1956), where it was referred to as an oceanographical curiosity. Only a few years later it was recognized as an important phenomenon with applications in several branches of science. Several early reviews of this topic were published (Turner, 1974, Huppert and Turner, 1981, Fernando and Brandt, 1994) and books on the subject are presently available (Brandt and Fernando, 1995, Radko, 2013). Double-diffusive convection is the flow originated by buoyancy in a fluid where two different density gradients are present, which have different diffusion rates**.** These flows occur in a wide variety of fields, such as oceanography, astrophysics, geophysics, solar energy and crystal growth, among others.

An example of double-diffusive convection occurs in salt gradient solar ponds (SGSP). An SGSP is a reservoir containing a mixture of salt and water, heated by solar radiation and used as a device to collect and store solar energy. In order to absorb radiation in the reservoir, it is necessary that the mixture is transparent enough for radiation to penetrate to the bottom. On the other hand, and in order to accumulate energy, thermal losses must be minimized. This can be achieved through appropriate coverage of the surface, insulation of the side and bottom walls, and inhibition of convective processes in the reservoir. The latter may be achieved by means of a salt gradient with a salinity close to zero at the surface and increasing towards the bottom. Since the construction is easy and the maintenance has a low cost, due to the use of common substances such as water and salt, this type of solar pond is the most widely studied and developed.

There are three distinct zones in an SGSP: a surface zone, an intermediate or gradient zone and a storage zone. The surface and the storage zones are essentially convective zones where the temperature may be considered uniform. They are usually referred to as upper convective zone (UCZ) and lower convective zone (LCZ), respectively. The former is a zone with low salt concentration that naturally develops as a result of outside effects such as wind, rain and heat exchange from the pond to the environment. The typical thickness of this zone ranges from 0.2 m to 0.5 m. The storage zone is used for absorption and storage of solar energy. The highest temperatures are attained in this region, whose thickness varies according to the amount of energy to be stored and the temperatures to be obtained. Typically, its thickness ranges from 0.5 m to 1.5 m. The intermediate zone, where heat transfer is only by conduction, behaves as a thermal insulator between the bottom and the surface. It is referred to as the non-convective zone (NCZ). In order to generate this NCZ, whose thickness ranges from 1 m to 2 m, an artificial salinity gradient is enforced to


doi:10.18086/swc.2019.07.01 Available at http://proceedings.ises.org

prevent convection and to allow the storage of the energy absorbed in the LCZ, from where it can be extracted for consumption.

The non-convective characteristics of the NCZ cannot be maintained indefinitely. Mechanical or thermal perturbations or double diffusion phenomena in this zone or at its borders contribute to destabilization. In particular, the phenomenon of double diffusion can contribute to the amplification of small disturbances due to the thermal diffusion coefficient being two orders of magnitude higher than the molecular diffusion. This phenomenon gives rise to movement, induced only by diffusion, which can then lead to convective flow.

Solar ponds may be used for several purposes, namely heating of buildings, industrial process heating, power production and desalination (El-Sebaii *et al*., 2011). The ability of ponds with a salinity gradient to store solar energy was firstly reported more than one hundred years ago, leading to the proposal of the construction of artificial solar ponds to use energy for domestic or industrial purposes. The first artificial pond was built about sixty years ago, while pioneering theoretical studies were published about fifty years ago. Indeed, the first attempts to model solar ponds date back to the sixties, and consist of analytical one-dimensional models. Models based on the numerical solution of the governing equations for mass, momentum, energy and salinity provide additional insight into the phenomena under investigation. Although one-dimensional models may be useful (e.g., Angeli and Leonard, 2005), probably being the most widely ones, multidimensional models give a far more detailed description of the underlying physical phenomena. However, only a few transient multidimensional studies have been reported in the literature.

El-Refaee *et al*. (1996) developed a two-dimensional mathematical model that uses the vorticity, dilatation, density, temperature and concentration as dependent variables. The transient thermal performance of the SGSP was predicted by solving numerically the governing equations using the finite difference method. Mansour *et al*. (2004) solved the 3D conservation equations for energy and salinity in an SGSP using the finite volume method, under the assumption that convection did not occur and only heat and mass diffusion took place during the simulation period. The thickness of the UCZ, NCZ and LCZ was fixed. They found that the pond stability was affected by absorption of solar radiation and by heat losses through the free surface. An investigation of the pond stability during a long period of time using real meteorological data was later reported for a 2D configuration (Mansour *et al*., 2006).

The first 3D simulation of a SGSP based on the solution of the conservations equations for mass, momentum, energy and salinity was presented by Jubran *et al*. (2004). They used the code PHOENICS, based on the finite volume method, to investigate the effects of the tilt angle of side walls and salt concentration on the onset of convective layers on the sidewalls of the pond. The hydrodynamic and thermal transient behaviour of an enclosure with vertical temperature and salinity gradients were modelled by Hammami *et al*. (2007) using the finite volume method to numerically solve the 2D governing equations for mass, momentum, energy and salinity. Milhazes *et al*. (2009) used a spectral method to solve the weak form of the same set of governing equations for an SGSP. They found that the predictions were improved by taking into account the dependence of the density and viscosity on the temperature and salinity. Suárez *et al*. (2010) used the commercial code Fluent to predict the performance of an SGSP during energy collection and storage. They employed a fully coupled transient 2D numerical model that is able to describe short and medium term operations, allowing the interfaces between the zones to dynamically adjust along the time. The absorption of solar radiation and the wind effect were taken into account.

Boudhiaf and Baccar (2014) extended the work of Hammami *et al*. (2007) and investigated the effect of the Rayleigh number on the thermal behavior of the pond and the effect of the aspect ratio on the temperature and velocity fields. Giestas *et al*. (2014) used the same mathematical model formerly reported by Milhazes *et al*. (2009) to simulate double diffusion in a rectangular cavity filled with a mixture of water and salt, which is heated at the bottom. However, they employed the finite element method rather than the spectral method to solve the governing equations. Their predictions were in reasonable agreement with experimental results, but the observed perturbations at the interface between the LCZ and the NCZ were barely visible and unstable in the numerical results. Giestas *et al*. (2016) applied this model as well as Ansys Fluent to the simulation of a lab-scale SGSP. They predicted well the main features of the relevant physical phenomena in the SGSP, including the temperature in the three different zones.

More recently, El Mansouri *et al*. (2017) developed a 2D hybrid finite volume – Lattice-Boltzmann method to study the thermal behavior and the energy efficiency of an SGSP. The same mathematical model was used to further study the transient thermal behaviour and stability of the pond (El Mansouri *et al*., 2018). Anagnostopoulos *et al*. (2017) used a more fundamental approach than in previous works to model the absorption of radiation in the pond, by means of the solution of the radiative transfer equation using the discrete ordinates method. Both 2D and 3D simulations were performed using the COMSOL software package. Recently, El-Kadi *et al*. (2019) used Ansys Fluent to simulate an SGSP in hot climate regions, and investigated the development and interactions of the three zones of the pond.

In the present work, the problem of double diffusion in a salt stratified fluid heated from below and characterized by conditions similar to those found in an SGSP is revisited. The influence of lateral cooling on the double diffusion, which was not accounted for by Giestas *et al*. (2014), is studied. Moreover, the ability of the model to predict relevant physical phenomena experimentally observed is investigated.

## 2. Mathematical modelling

The mathematical model is based on the governing equations for conservation of mass, momentum, energy and salt mass fraction. The fluid is Newtonian and the diffusion of energy and mass satisfy the Fourier and Fick's laws, respectively. The Boussinesq approximation is employed, so that the density is assumed to be constant except in the buoyancy term, where it is linearly related to the temperature and to the salt concentration. The governing equations may be written as follows:

$$\nabla \cdot \mathbf{v} = 0 \tag{1}$$

$$\frac{\partial \mathbf{v}}{\partial t} + \mathbf{v}.\nabla\mathbf{v} = -\frac{\nabla p}{\rho_o} + \nu \Delta\mathbf{v} + \mathbf{f} \tag{2}$$

$$\frac{\partial T}{\partial t} + \mathbf{v}.\nabla T = \alpha \Delta T \tag{3}$$

$$\frac{\partial S}{\partial t} + \mathbf{v}.\nabla S = D_s \Delta S \tag{4}$$

In these equations, $\mathbf{v}$ is the velocity vector, $T$ the temperature, $S$ the mass fraction of salt (salinity), $\rho_o$ the density calculated at reference values of temperature and salinity, $p$ the pressure, $t$ the time, $\nu$ the kinematic viscosity, $\alpha$ the thermal diffusivity and $D_S$ the salt diffusion coefficient. The vector $\mathbf{f}$ is defined as

$$\mathbf{f} = \left[1 - \beta_T\left(T - T_o\right) + \beta_S\left(S - S_o\right)\right]\mathbf{g} \tag{5}$$

where $\mathbf{g}$ is the acceleration of gravity vector, $T_o$ and $S_o$ are reference values of temperature and salinity, respectively, $\beta_T$, is the thermal expansion coefficient, and $\beta_S$ the salinity contraction coefficient.

The spatial discretization was carried out using the Galerkin finite element formulation. Bilinear elements were employed for the pressure and biquadratic elements were used for the velocity, temperature and salt mass fraction. The time discretization was performed using a second-order backward differencing scheme with a backward Euler method being employed for the first time step. The energy and salt mass fraction equations are dominated by advection, and therefore lack stability when discretized using Galerkin type methods and may yield spurious oscillations or wiggles. In order to overcome this problem, stabilization methods are usually employed. Several stabilization methods may be used to overcome this difficulty and in the present work the method of Almeida and Silva (1997) is used. This is a spurious oscillation at layers diminishing method that adds isotropic artificial diffusion to the streamline upwind Petrov-Galerkin stabilization term.

In each time step, the governing equation for energy is solved first, followed by the salt mass fraction transport equation and the Navier-Stokes equations. The Navier-Stokes equations are solved using a sequential operator splitting method to handle the velocity and pressure coupling. In the first substep, an intermediate velocity field is obtained using a guessed pressure field, while in the second substep a Poisson equation for the pressure with homogeneous Neumann boundary conditions is solved. Then, the pressure is updated and the divergence free velocity field is computed using the guessed and the updated pressure. Details of the solution algorithm may be found in Giestas *et al*. (2014). The time step was adaptively controlled using the method proposed by Jonhson *et al*. (1990). The system of discretized linear equations resulting from the space and time discretization of the governing equations was solved using the conjugate gradient method with ILU(0) preconditioning.

The deal.II open source finite element library (Bangerth *et al*., 2007) was employed in the present work. This library allows the parallelization of the code using threading building blocks (TBB). TBB is a software template library developed by Intel for task-based shared memory parallel programming on multicore processors. The basic linear algebra operations are parallelized using the available libraries, but the user needs to define other types of parallelization, such as the assembling of the global matrices and the solution of the system of linear algebraic equations. The calculation of the local element matrices and the assembling of these matrices are parallelized.

## 3. Results and discussion

Double diffusion of a salt stratified fluid heated from below is simulated in the present work. The simulations reproduce the experimental conditions of a previous study performed in a laboratory plexiglass rectangular box with a width of 5 cm and a height of 10 cm (Tavares, 2010). The density, the kinematic viscosity, the thermal and the salinity diffusion coefficients, and the thermal expansion and salinity contraction coefficients were evaluated at the average temperature (30ºC) and average salinity (25 g/kg), yielding: $\rho$=1.024×10$^3$ kg/m$^{-3}$, $\nu$= 0.805×10$^6$ m$^2$ s$^{-1}$, $\alpha$ = 1.6×10$^{-7}$ m$^2$ s$^{-1}$, $D_s$=1.64×10$^{-9}$ m$^2$ s$^{-1}$, $\beta_T$=3.35×10$^{-4}$ K$^{-1}$, $\beta_S$=6.65×10$^{-4}$ kg g$^{-1}$. The fluid is initially at rest, the initial temperature is equal to the ambient air temperature (22.95 ºC), which is assumed to remain constant, and the initial salt mass fraction decreases linearly from 51.2 g/kg at the bottom to 12.3 g/kg at a height of 0.085 cm and remains constant further up.

The velocity is equal to zero at the bottom and side boundaries, and a zero velocity gradient is prescribed at the free surface on the top boundary. Convective heat transfer and a zero salinity gradient are prescribed at all the boundaries. The convective heat transfer coefficient tis equal to 10 W m$^{-2}$ K$^{-1}$ at the top and side boundaries, and 320 W m$^{-2}$ K$^{-1}$ at the bottom boundary. The temperature of bottom boundary is set to 50 ºC. Past calculations (Giestas *et al.*, 2014) have revealed several shortcomings. Therefore, radiative heat losses through the side walls are also considered in the present work. It is assumed that the surrounding temperature is equal to the ambient temperature, the emissivity of the outer surface of the box is 0.984 and the thermal resistance of the wall of the box is negligible. The calculations were carried out using a uniform mesh with 70×140 elements along with an adaptive time step, the maximum time step being limited to 0.06 s.

The results obtained at $t$=540 s are illustrated in Fig. 1. On the left, the predicted velocity field is overlapped with a Schlieren image and, on the right, the vertical profiles of density and salt mass fraction are plotted at a distance from the right wall of 0.5 cm. The relative change in light intensity (grey scale) in the Schlieren image corresponds to changes in the density gradient. The density and the salinity profiles show that the predicted location of the interfaces between the UCZ and the NCZ, and between the NCZ and the LCZ, is in good agreement with that image. The lower and upper convective zones, denoted by LCZ and UCZ, respectively, are well defined, as evidenced by the uniform temperature and salinity profiles at the lower and upper regions in Fig. 1, respectively. At the interface that separates the LCZ from the non-convective zone (NCZ), there is a steep gradient of density and salinity with a thickness of

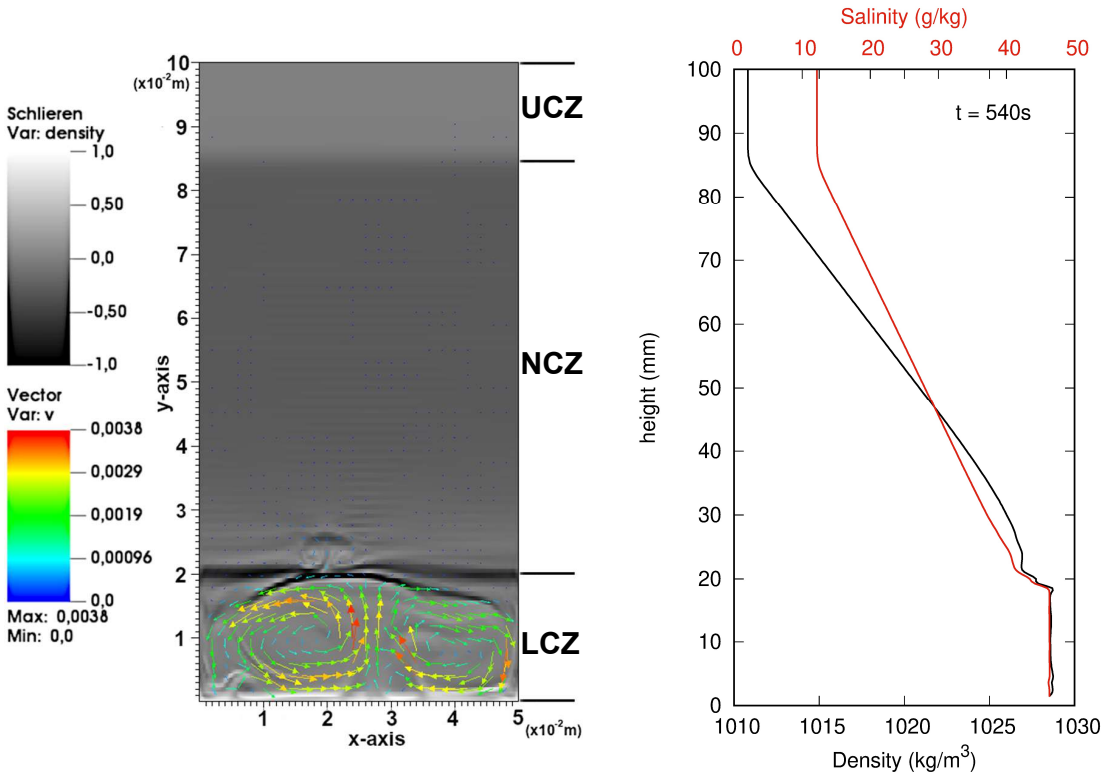


**Fig. 1: Predicted velocity field overlapping a Schlieren image at $t$=540 s (left) along with vertical density and salinity profiles at a distance of 0.5 cm from the right wall.**

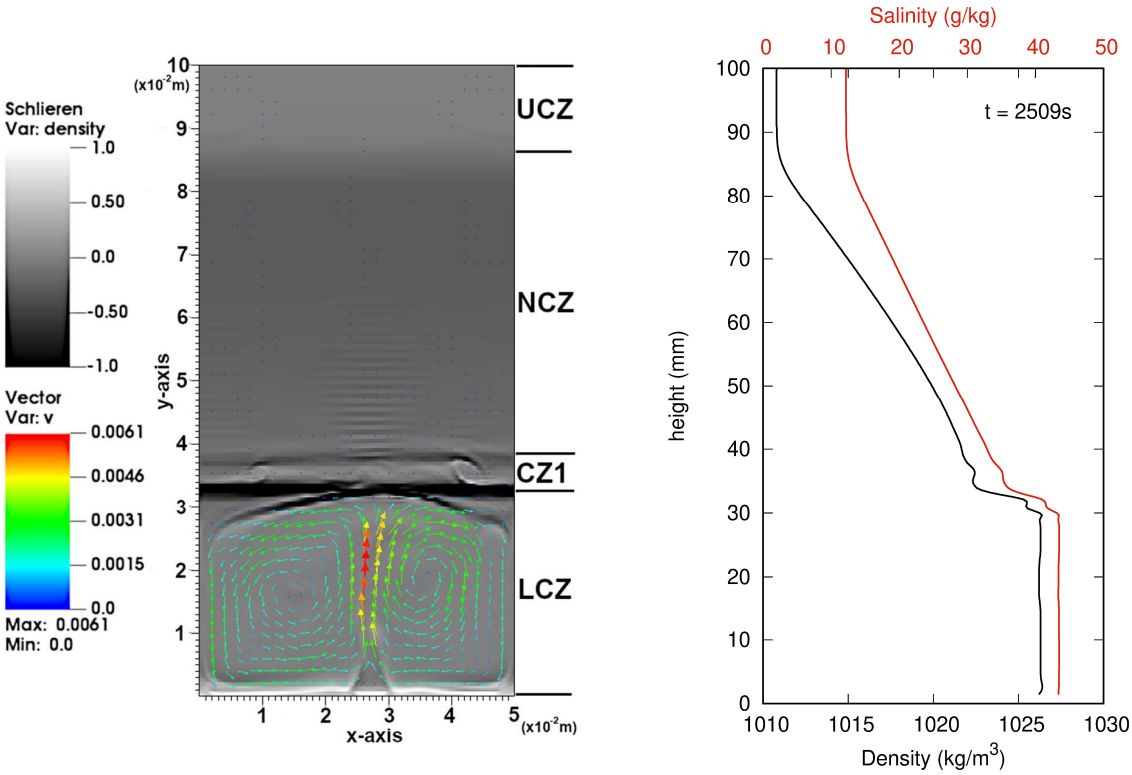


**Fig. 2: Predicted velocity field overlapping a Schlieren image at *t*=2509 s (left) along with vertical density and salinity profiles at a distance of 0.5 cm from the right wall.**

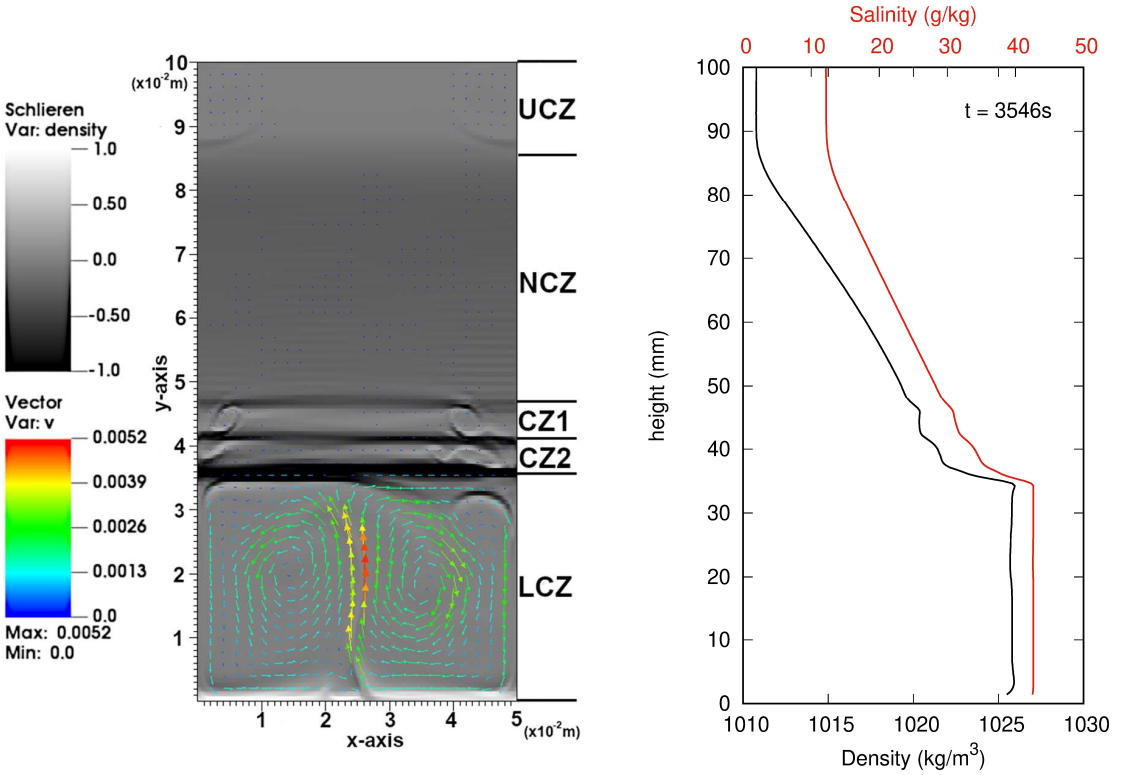


**Fig. 3: Predicted velocity field overlapping a Schlieren image at *t*=3546 s (left) along with vertical density and salinity profiles at a distance of 0.5 cm from the right wall.**

about 3 mm. A perturbation above that interface that extends up to about 2.5 cm can also be seen. The transport of heat and mass across the interface takes place when the momentum of a rising plume of hot fluid is high enough to penetrate through the interface. This instability mechanism is observed when the LCZ is still being formed and is not thick enough to absorb the kinetic energy of the rising hot fluid and to prevent the disruption of the interface. Immediately below the interface between the LCZ and the NCZ, the velocity field and the vertical density and salinity profiles shown in Fig. 1 reveal the transport of fluid of high salinity from the LCZ to the interface and of fluid of lower salinity from the interface to the LCZ. The salinity gradient in the NCZ is constant, while that of density is only linear at a height greater than about 5 cm from the bottom.

The system continues to evolve with an increase of the height of the LCZ and the sporadic appearance of disturbances, as seen in Fig. 1. At $t$=2509 s, a second well-defined convective zone (CZ1) of relatively small height is visible in Fig. 2. The location of the interfaces between neighbouring zones evidenced by the density and salinity profiles is again confirmed by the Schlieren image. In the CZ1, rolls spinning in clockwise direction next to right side wall and anticlockwise direction close to the left wall can be observed. The appearance of these rolls was also reported by Lee and Hyun (1991) and Kranenborg and Dijkstra (1998) in the experiments of dual-diffusion with side cooling. The density and salinity vertical profiles exhibit small oscillations in the transition between the LCZ and the CZ1, as well as between the CZ1 and the NCZ. The homogeneity is visible in both the LCZ and the UCZ.

At time instant $t$=3546 s, Fig. 3 shows the presence of two convective zones above the LCZ, i.e. a second convective zone, CZ2, formed adjacent to the previously existing zone, CZ1. The Schlieren image confirms the numerical predictions. The thickness of these two zones is approximately the same, but the rolls in the CZ2 are more well-defined than in the CZ1. Although there is flow motion in these two layers, the computed velocities are very small, being of the order of tenths of millimeters per second. The beginning of flow motion in the UCZ and the variation of density suggest that there is transfer of mass and heat by convection in that zone. The density and salinity profiles reveal that the thickness of the LCZ is about 3.5 cm, while that of the NCZ is about 4 cm. The interfaces between the LCZ-CZ1, CZ1-CZ2 and CZ2-NCZ zones correspond to the abrupt changes of density/salinity observed in those profiles at a height between 3.5 cm and 4.5 cm. There is no velocity in the NCZ, so that only heat and mass diffusion take place in this region, and there is no transport by convection or the emergence of disturbances. The UCZ is rather homogeneous, but in addition to heat and mass diffusion, the Schlieren image discloses a slight density variation in the vicinity of the side walls and close to the bottom of this zone.

At $t$=4596 s, Fig. 4 shows that the CZ2, which was visible in Fig. 3, collapsed and only the intermediate layer CZ1 is now present between the LCZ and the NCZ. As a result, there is a single convective zone with a thickness of about 1 cm above the LCZ. The fluid in the rolls observed in the CZ1 moves as expected in the case of lateral cooling, i.e. in anticlockwise direction close to the left wall and in clockwise direction close to the right wall. The velocity in the UCZ is now visible, contributing to the transport of heat and mass. The density and the salinity profiles show a LCZ with a thickness of about 4 cm and a NCZ of 3.5 cm thickness. The steep gradients observed in both profiles at the interfaces between the LCZ and the CZ1, as well as the interface between the CZ1 and the NCZ, prove that the CZ1 is well-defined and stable. It is quite clear that the CZ1 is a convective layer, since the density and salinity are homogeneous in this zone.

The Schlieren's image in Fig. 5 reveals that an interface was formed that split the CZ1 observed in Fig. 4 into two zones, which are referred to as CZ1 and CZ2. The variation in density and the velocity field at the top of the LCZ suggest the transport of salinity from the interface between that zone and the CZ1 in counterclockwise direction. A similar transport phenomenon can be seen at the UCZ, next to the interface with the NCZ, with counterclockwise direction close to the left wall and with clockwise direction near the right wall. The vertical profiles of density and salinity reveal a homogeneous LCZ and a linear variation of density and salinity in the NCZ. Small steps are visible in these profiles at the interfaces of neighbouring zones. Moreover, the smooth gradient at the interfaces of the CZ1 and the CZ2 suggests that these zones are unstable.

There is a gradual increase of the thickness of the UCZ, as one can conclude by comparing Figs. 5 and 6, as well as a marginal increase of the velocity in that zone, although not significant compared to the velocity observed at the LCZ. At $t$=9693 s, the unstable CZ1 and CZ2 layers are no longer visible, which means that they collapsed, and only the three typical zones of a SGSP are present. The thickness of the LCZ increased to about 5 cm, while that of the NCZ decreased to 3 cm. The flow is stronger in the LCZ, the maximum velocity being 6.8 mm $s^{-1}$. The transport of salt is visible at both the interface between the LCZ and the NCZ and at that between the NCZ and the UCZ. The flow in this latter zone is now more intense and the transport of salinity to the UCZ yielded an increase of its thickness, which is about 2 cm. The gradients of salinity and density at the interface between the LCZ and the NCZ are larger, which suggests a greater stability of that interface. Both the salinity and the density profiles are linear in the NCZ.

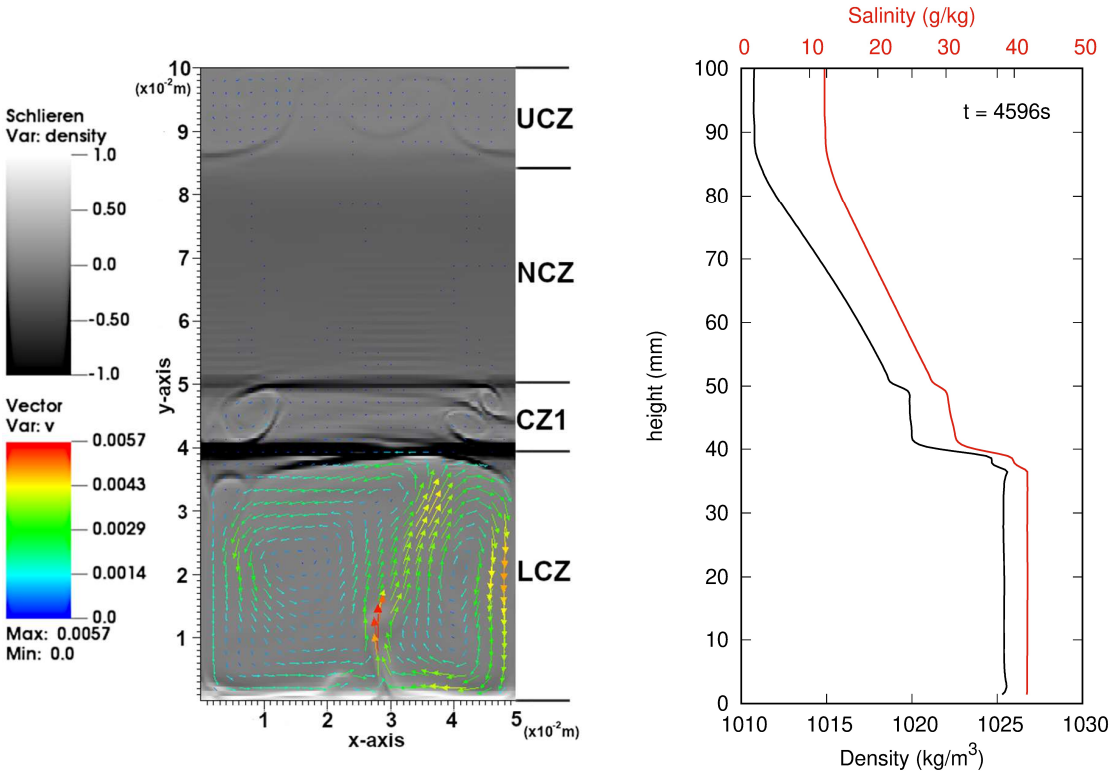


**Fig. 4: Predicted velocity field overlapping a Schlieren image at *t*=4596 s (left) along with vertical density and salinity profiles at a distance of 0.5 cm from the right wall.**

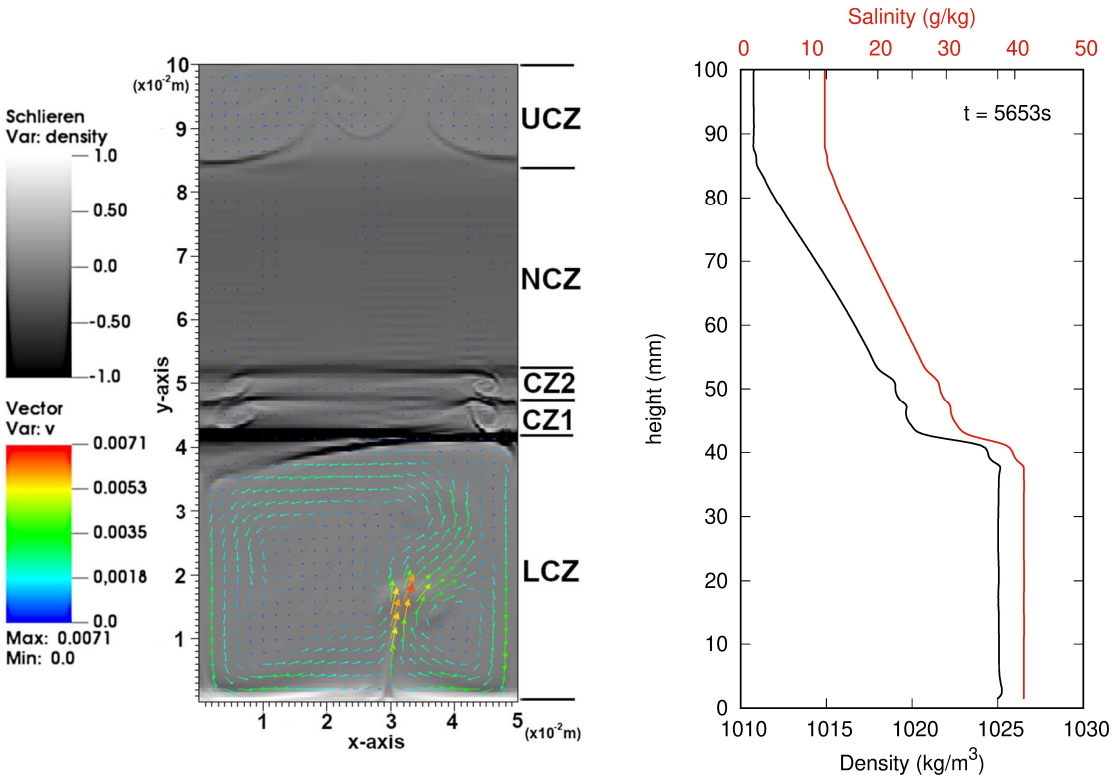


**Fig. 5: Predicted velocity field overlapping a Schlieren image at *t*=5653 s (left) along with vertical density and salinity profiles at a distance of 0.5 cm from the right wall.**

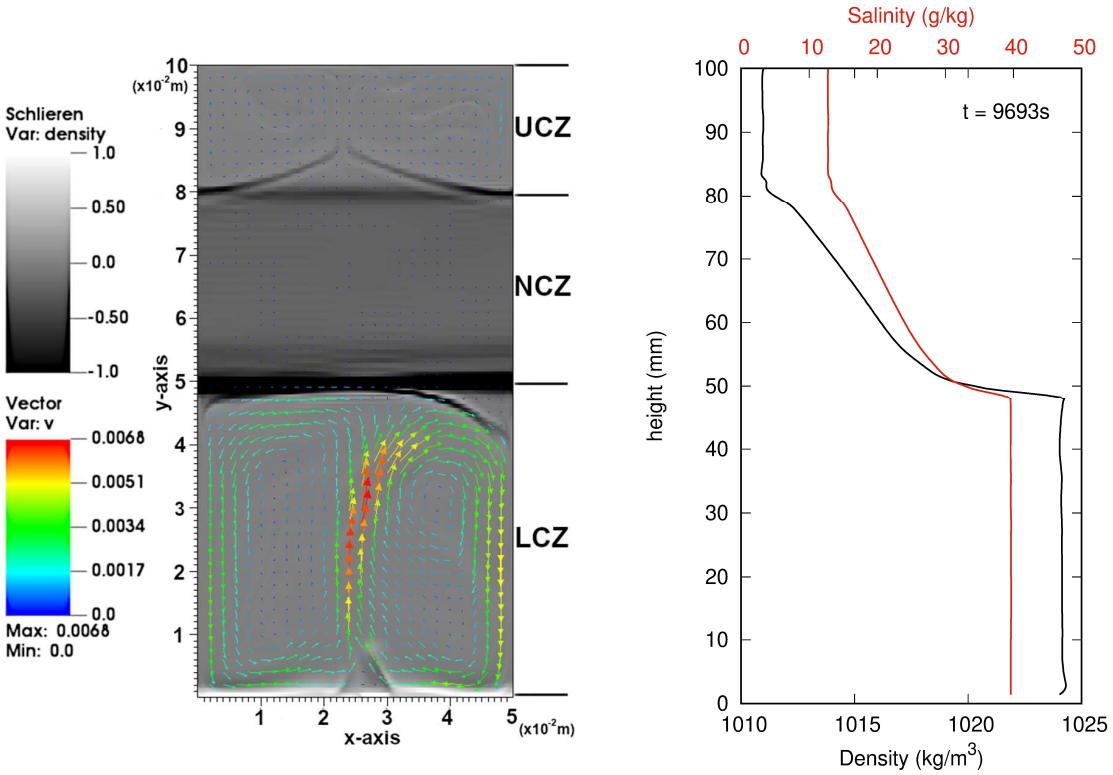


**Fig. 6: Predicted velocity field overlapping a Schlieren image at *t*=9693 s (left) along with vertical density and salinity profiles at a distance of 0.5 cm from the right wall.**

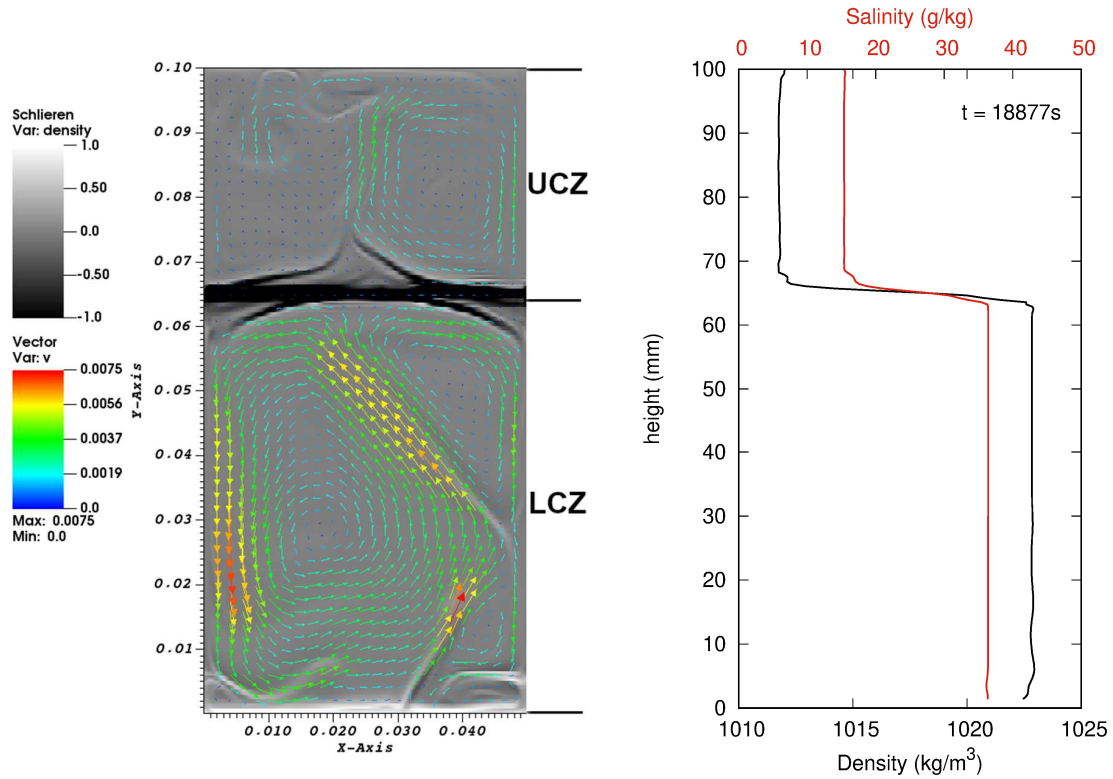


**Fig. 7: Predicted velocity field overlapping a Schlieren image at *t*=18,877 s (left) along with vertical density and salinity profiles at a distance of 0.5 cm from the right wall.**

Figure 7 shows the NCZ has disappeared at $t$=18,877 s, i.e, at a time that is almost twice the instant of time considered in the previous figure. The only remaining interface is the one that separates the LCZ from the UCZ and is very well defined. The average velocities at the UCZ and the LCZ are 4.5 and 2.1 mm $s^{-1}$, respectively. The convective cells in the UCZ are not as well defined as before, and their configuration in the LCZ often changes in time. The steep gradients of salinity and density at the interface between the two zones reveal that the interface is very stable.

## 4. Conclusions

The analysis carried out in a salt stratified fluid heated from below allowed the identification of several physical phenomena, e.g., the heat and mass transport across a diffusive interface, the disruption of an interface and the role of lateral cooling on double diffusive convection. The appearance of secondary convective zones above the LCZ experimentally observed during some time is well reproduced by the numerical simulation. The prediction of the location of these zones is in agreement with the experimental data. Occasionally, the disruption of the interface takes place and then the colder and less salty fluid in the NCZ flows to the LCZ causing an instability. As the equilibrium is restored, a thin layer of fluid with salinity and temperature slightly higher than those of the adjacent fluid appears right above the region where the plume crossed the interface. The lateral cooling originates inner convective zones in the NCZ that arise when the LCZ is thick enough such that the transport mechanism across the diffusive interface does not destroy the density stratification pattern.

## 5. Acknowledgements

The support of the Portuguese Science Foundation (FCT) through IDMEC, under LAETA, project UID/EMS/50022/2019 is acknowledged.

## 6. References

Anagnostopoulos, A., Campbell, A., Arellano-Garcia, H., 2017. Modelling of the thermal performance of SGSP using COMSOL multiphysics. Computer Aided Chemical Engineering. 40, 2575-2580.

Almeida, R.C., Silva, R.S., 1997. A stable Petrov-Galerkin method for convection-dominated problems. Comp. Methods Appl. Mech. Engrg. 140, 291-304.

Angeli. C., Leonard, E., 2004. A one dimensional numerical study of the salt diffusion in a salinity gradient solar pond. Int. J. Heat Mass Transfer, 47, 1-10.

Bangerth, W., Hartmann, R., Kanschat, G., 2007. deal.II — A general-purpose object-oriented finite element library. ACM Trans. Math. Softw. 33, Article 4.

Boudhiaf, R., Baccar, M., 2014. Transient hydrodynamic, heat and mass transfer in a salinity gradient solar pond: a numerical study. Energy Convers Manag. 79, 568–580.

Brandt, A., Fernando, H.J.S. (Eds.) 1995. Double-Diffusive Convection. Wiley, Washington, DC.

El Kadi, K., Elagroudy, S., Janajreh, I., 2019. Flow simulation and assessment of a salinity gradient solar pond development. Energy Procedia 158, 911-917.

El Mansouri, A., Hasnaoui, M., Bennacer, R., Amahmid, A., 2017. Transient thermal performance of a salt gradient solar pond under semi-arid Moroccan climate using a double-diffusive convection model. Energy Convers Manag. 151, 199-208.

El Mansouri, A., Hasnaoui, M., Amahmid, A., Bennacer, R., 2018. Transient modeling of a salt gradient solar pond using a hybrid finite-volume and cascaded Lattice-Boltzmann method: Thermal characteristics and stability analysis. Energy Convers Manag. 158, 416-429.

El-Refaee, M.M., Mansour, R.R., Al-Juwayhel, F., 1996. Transient performance of a two-dimensional salt gradient solar pond – a numerical study. Int. J. Energy Research. 20, 713-731.

El-Sebaii, A.A., Ramadan, M.R.I., Aboul-Enein, S., Khallaf, A.M., 2011. History of the solar ponds: A review study. Renew. Sustain. Energy Rev. 15, 3319-3325.

Fernando, H.J.S., Brandt, A,. 1994. Recent advances in double-diffusive convection. Appl. Mech. Rev. 47, c1-c7.

Giestas, M.C., Milhazes, J.P., Pina, H.L., 2014. Numerical modeling of solar ponds. Energy Procedia. 57, 2416-

2425.

Giestas, M.C., Milhazes, J.P., Coelho, P.J., Joyce, A.M., Loureiro, D., 2016. CFD modeling of a small case solar pond. Conference Proceedings EuroSun 2016, Palma de Mallorca, Spain, 11-14 October.

Hammami, M., Mseddi, M., Baccar, M., 2007. Transient natural convection in an enclosure with vertical solutal gradients. Solar Energy, 81, 476-487.

Huppert, H.E., Turner, J.S., 1981. Double-diffusive convection. J. Fluid Mech., 106, 299-329.

Johnson, C., Nie, Y.-Y., Thomée, V., 1990. An a posteriori error estimate and adaptive timestep control for a backward euler discretization of a parabolic problem. SIAM J. Numer. Anal. 27, 277–291.

Jubran, B.A., Al-Abdali, H., Al-Hiddabi, S., Al-Hinai, H., Zurigat, Y., 2004. Numerical modelling of convective layers in solar ponds. Solar Energy, 77, 339-345.

Kranenborg, E.J., Dijkstra, H.A., 1998. On the evolution of double-diffusive intrusions into a stably stratified liquid: a study of the layer merging process. Int. J. Heat Mass Transfer. 41, 2743-2756.

Lee, J.W., Hyun, J.M., 1991. Time-dependent double diffusion in a stably stratified under lateral heating. Int. J. Heat Mass Transfer, 34, 2409-2421.

Mansour, R.B., Nguyen, C.T., Galanis, N., 2004. Numerical study of transient heat and mass transfer and stability in a salt-gradient solar pond. Int. J. Thermal Sciences, 43, 779-790.

Mansour, R.B., Nguyen, C.T., Galanis, N., 2006. Transient heat and mass transfer and long-term stability of a salt-gradient solar pond. Mechanics Research Communications, 33, 233-249.

Milhazes, J.P., Giestas, M.C., Pina, H.L., Tavares, C., 2009. Solar pond modeling with density and viscosity dependent on temperature and salinity. Int. J. Heat and Mass Transfer, 52:2849-2857.

Radko, T., 2013. Double-Diffusive Convection. Cambridge University Press, Cambridge.

Stommel, H., Arons, A.B., Blanchard, D., 1956. An oceanographical curiosity: the perpetual salt fountain. Deep Sea Research, 3, 152-153.

Suárez, F., Tyler, S.W., Childress, A.E., 2010. A fully coupled, transient double-diffusive convective model for salt-gradient solar ponds. Int. J. Heat and Mass Transfer, 53, 1718-1730.

Tavares, C., 2010. Estudo Experimental da Dinâmica de Dupla-Difusão Calor-Massa num Meio Estratificado (in Portuguese). Ph.D. Thesis, Technical University of Lisbon.

Turner, J.S., 1974. Double-diffusive phenomena. Ann. Rev. Fluid Mech. 6, 37-56.